Hindawi
Journal of Chemistry
Volume 2022, Article ID 5101712, 9 pages
https://doi.org/10.1155/2022/5101712

Research Article

Hemoglobin I from *Lucina pectinata* on Collagen Scaffold: A Prospective Hydrogen Sulfide Scavenger

Jennifer Vargas Santiago,[1] **Anibal Quintana Cheeseborough**,[2] **and Juan López-Garriga**[1,3]

[1]*Department of Chemistry, P.O. Box 9000, University of Puerto Rico at Mayaguez Campus, Mayaguez, PR 00681-9000, USA*
[2]*Integra LifeScience Corp., P.O. Box 167, Añasco, PR 00610, USA*
[3]*Industrial Biotechnology Program, P.O. Box 9000, University of Puerto Rico at Mayaguez Campus, Mayaguez, PR 00681-9000, USA*

Correspondence should be addressed to Juan López-Garriga; juan.lopez16@upr.edu

Received 21 January 2022; Revised 9 April 2022; Accepted 16 April 2022; Published 4 May 2022

Academic Editor: Mohd. Sajid Ali

Hydrogen sulfide (H_2S), independently of being a toxic gas with a characteristic smell of rotten eggs, is a crucial signaling molecule with significant physiological functions. Given the rapid diffusivity of the gas, it is a challenge to develop robust sensors and biomarkers to quantify free or bound H_2S. In addition, there is the need to further develop a robust biosystem to efficiently trap or scavenge H_2S from different producing environments. The work presented here uses recombinant met-aquo rHbI (rHbI-H_2O) immobilization techniques on collagen to determine its ability to bind H_2S due to its high affinity ($1.24 \times 10^8\ M^{-1}$). The hemeprotein will function as a scavenger on this scaffold system. UV-Vis absorption and UV-Vis diffuse reflectance (%R) spectroscopy of rHbI-H_2O and rHbI-sulfide (rHbI-H_2S) complex in solution and collagen scaffold demonstrated that the heme chromophore retains its reactivity and properties. UV-Vis diffuse reflectance measurements, transformed using the Kubelka-Munk function (K-M function), show a linear correlation ($R_2 = 0.9987$ and 0.9916) of rHbI-H_2O and rHbI-H_2S within concentrations from 1 μM to 35 μM for derivatives. The extraordinary affinity of rHbI-H_2O for H_2S suggests recombinant met-aquo HbI in a collagen scaffold is an excellent scavenger moiety for hydrogen sulfide. These findings give insight into H_2S trapping using the rHbI-H_2O-collagen scaffold, where the rHbI-H_2S concentration can be determined. Future pathways are to work toward the development of a met-aquo rHbI collagen solution capable of being printed as single drops on polymer, cotton or chromatographic paper. Upon exposure of these matrixes to H_2S, the rHbI-H_2S complex is formed and its concentration determined using UV-Vis diffuse reflectance technique.

1. Introduction

Human physiology is influenced by exogenous hydrogen sulfide (H_2S) at higher concentrations than 300 μM leading to death at 15 mM [1, 2]. However, significant discoveries suggest the endogenous synthesis of H_2S in mammalians. Desulfuration of cysteine, homocysteine, and cystathionine by the enzymes cystathionine β-szynthase (CBS), cystathionine ɣ-lyase (CSE), D-amino acid oxidase (DAO), and indirectly by 3-mercaptopyruvate sulfurtransferase (3-MST) produces H_2S in the body [3]. The amount generated can range from 10 to 300 μM or lower depending on enzyme distribution in the particular tissue [4–6]. H_2S plasma values that vary between 50 and 150 μM are associated with several conditions [4]. For instance, SARS-CoV-2 survivors show serum H_2S levels higher (≥150 μM) than those nonsurvivors [7]. Overexpressed CSE in the pancreas increases H_2S levels, inducing the pathogenesis of diabetes in rats [8]. In contrast, reduction in the enzymatic activity of CSE promoted hypertension in rats and women with preeclampsia [9, 10]. Reduced H_2S levels are also related to Parkinson's, Alzheimer's, and atherosclerosis disease [11, 12]. Despite this

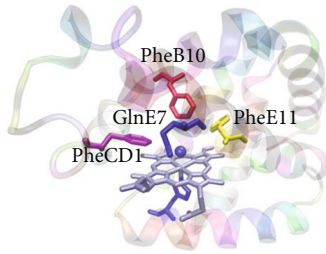

Figure 1: Tertiary structure and the heme active site of the HbI from *Lucina pectinata* (PDB:1MOH). The active site shows the amino acid around the heme group.

knowledge, fundamental questions and concerns remain. For example, H_2S concentration values are subject of intense dispute because there is no suitable robust sensor capable of directly measuring H_2S in tissues and plasma [13]. Therefore, an attractive alternative is the development of an H_2S acceptor that can efficiently trap hydrogen sulfide gas from biological samples for detection and quantification.

Hydrogen sulfide is a lipophilic molecule that can diffuse through membranes without facilitating membrane channels [10]. At pH 7.4, there is approximately 80% HS^- and 20% H_2S. Hydrogen sulfide solubility is (~113 mM, 86 mM, and 68 mM at 20°C, 30°C, and 40°C, respectively) a function of temperature; hence, determining this gas concentration is complicated [14]. Therefore, the hydrogen sulfide generation rate, turnover, concentration, identification, products, transport, and concentration remain a significant challenge in tissues, organs, and plasma. The methylene blue method is the standard procedure for the quantitative determination of hydrogen sulfide, but its application is restricted to solutions using hazardous reagents [13]. Also, amperometric sensors have been reported for H_2S detection [15–18], being the polarographic hydrogen sulfide sensor (PHSS) one of the most cited [19].

The recombinant hemoglobin I (rHbI) from the clam *Lucina pectinata* (Figure 1) with the heme in the Fe^{III} oxidation state has an extraordinary affinity for H_2S (k_{on} 6.8×10^3 M^{-1} s^{-1}/k_{off} 5.5×10^{-5} s^{-1}) of 1.24×10^8 M^{-1}, which makes met-aquo rHbI exceptionally suitable for the detection of H_2S [20]. Therefore, the underlying hypothesis is that recombinant met-aquo HbI (rHbI-H_2O) collagen scaffold moiety could be a robust biosystem to efficiently trap or scavenge H_2S from solution. Although previous literature has supported that rHbI can trap the H_2S in different systems, its immobilization on collagen has not been yet studied. Previously, hemoglobin I had been immobilized as hexa-histidine tag rHbI in two gold electrodes detecting 25 to 800 nM H_2S in solution [21, 22]. Additionally, immobilization of hexa-lysine tag rHbI on carbon nanotubes via covalent conjugation showed a solution electrochemical response toward 10 to 300 μM H_2S [23]. Simultaneously, efforts have measured H_2S as gas evolving from a biological system. For example, a silver/Nafion/polyvinylpyrrolidone (PVP) membrane on a polystyrene microplate array was used to quantify H_2S from live glioma cells [24]. Furthermore, PVP membranes containing silver/Nafion were printed on chromatography paper to detect H_2S in live cell cultures [16, 25]. Gold/Silver-iodide dimeric nanoparticles were immobilized in agarose gel to create test strips capable of measuring H_2S from HepG2 cells with good sensitivity (500 nM), selectivity, and stability [26]. met-aquo rHbI encapsulated in tetramethyl orthosilicate (TMOS) sol-gel accepts hydrogen sulfide liberated from the rHbI-H_2S complex in solution, k_{off} 1.90×10^{-4} s^{-1}, revealing that met-aquo rHbI in TMOS is an effective trap for H_2S [27].

However, despite their advantages, TMOS sol-gels are difficult to work with and maintain in an overturned position [27]. This is not the case for collagen-based matrices, which have been used as assemblies to develop applications, such as tissue engineering, drug delivery, and biosensors [28–34]. For example, a collagen-based electroconductive hydrogel was used to prove the concept of an injectable sensor of glucose *in vivo* and tissues [28]. Also, colorimetric data of collagen and gold nanoparticles moieties were used to detect glucose in a linear range of 3 to 25 mM [35]. Moreover, *in vivo* oxygenation for skin wounds in diabetic mice was tracked using a collagen-dextran conjugated with a phosphorescence oxygen sensor [36]. Furthermore, a peroxide biosensor was constructed upon the encapsulation of hemoglobin in a ZrO_2-grafted collagen scaffold [37]. In contrast, a collagen hydrogel containing JK1, an H_2S releaser, was developed to deliver H_2S as a treatment for intervertebral disc degeneration [38]. Similarly, research has also been focused on developing matrixes to immobilize other H_2S-donors, e.g., JK2 and GYY4137, to release hydrogen sulfide from silk fibroin scaffold [39, 40], fibrous membranes [41], polymers [42], and sodium alginate sponges [43]. These systems have been created to mimic physiological release and proposed as alternatives to H_2S therapies.

The work presented here takes advantage of collagen versatility. A met-aquo rHbI collagen scaffold was constructed from a collagen sponge as an immobilization matrix for met-aquo Mb (Mb-H_2O), met-aquo rHbI (rHbI-H_2O), and rHbI-sulfide (rHbI-H_2S) species. The scaffold hemeprotein complexes were analyzed with UV-Vis absorption and UV-Vis diffuse reflectance measurements (R%) represented by the Kubelka-Munk function.

2. Materials and Methods

2.1. Sample Preparation. The recombinant His-tagged hemoglobin I was expressed in *Escherichia coli* Bli5 cells and purified as previously detailed in the literature [20, 44, 45]. Briefly, the expression was conducted using Terrific Broth supplemented with 30 μg/ml hemin chloride and 1% glucose. Protein expression was induced with 0.001 M isopropyl β-D-1-thiogalacto-pyranoside (IPTG) at 30°C and yielded red cell pellets, which were eventually lysed and centrifuged. The soluble protein fraction was purified using Co^{2+} affinity columns (Talon, Invitrogen) followed by fast performance liquid chromatography (FPLC) in a Hi Load 26/60 Superdex 200 gel filtration column with an automated AKTA FPLC System (Amersham Biosciences). Sodium dodecyl sulfate-polyacrylamide gel electrophoresis (SDS-PAGE) stained with Coomassie blue was performed on the purified protein. One band around 17 kDa confirmed the

purity and integrity of the hexa-histidine tag rHbI [44]. The met-aquo rHbI and met-aquo Mb from equine skeletal muscle were prepared by heme oxidation, adding a 10% molar excess of potassium ferricyanide. After the reaction, the oxidant was removed with a centrifugal filter (Pall Corporation). Solutions containing from 1 to 35 μM of met-aquo derivatives have been prepared by transferring different aliquots (1-70 μL) of 0.3 mM stock solution to 1 cm square quartz cuvettes (Starna Scientific) filled with buffer. The H_2S stock solution was prepared by dissolving Na_2S•9 H_2O salt in an amber vial and completed until 1.5 mL with buffer. Aqueous solutions were prepared with buffer containing 100 mM succinic acid, 100 mM potassium dihydrogen phosphate, and 1 mM ethylenediaminetetraacetic acid (EDTA) and adjusted to pH 6.5. The Na_2S•9 H_2O salt and buffer were purged and degassed before mixing to prevent oxygen contamination. Integra Life Sciences donated ultrapure lyophilized collagen sponges derived from the bovine tendon. Terrific Broth, hemin chloride, glucose ($C_6H_{12}O_6$, ≥99.5%), isopropyl β-D-1-thiogalacto-pyranoside (IPTG, ≥99%), myoglobin from equine skeletal muscle (Mb, ≥95-100%), potassium ferricyanide ($K_3[Fe(CN)_6]$, ACS reagent, ≥99.0%), sodium sulfide nonahydrate (Na_2S•9 H_2O, ≥99.99%), succinic acid ($C_4H_6O_4$, ≥99.0%), potassium dihydrogen phosphate (KH_2PO_4, ACS Reagent, ≥98.0%), and ethylenediaminetetraacetic acid (EDTA, ≥99.0%) were supplied by Sigma-Aldrich (USA) and used as received.

2.2. Hemeprotein Immobilization on Collagen Sponge. Immobilization of met-aquo Mb and met-aquo rHbI solutions was achieved individually by depositing 40 μL of protein solution (1-35 μM) onto the center of a collagen sponge with 2.0 × 2.0 × 0.2 cm in length, width, and height (thickness), respectively. All protein immobilization was done aerobically at 25°C. The collagen significantly reduced thickness where the hemeproteins drop solution was added. Thus, thickness size measurements were done on the spot for the met-aquo Mb and met-aquo rHbI collagen scaffold moieties. Ten samples were analyzed for the spot thickness (height) of the proteins collagen scaffold composite using a Leica MZ16 stereomicroscope coupled with a Nikon Digital Sight DS-5Mc-U1 camera. Each measure was repeated ten times for each sample, and a standard deviation was calculated for accuracy. The results showed that collagen with immobilized heme proteins had an average spot thickness of 0.041 cm. The rHbI-H_2S complex was prepared by adding 6 μL of 3.7 mM H_2S stock solution, equivalent to 482 μM, to the met-aquo rHbI collagen scaffold. Thus, the hydrogen sulfide ratio to met-aquo rHbI concentrations (1-35 μM) was 482 to 14.

2.3. Absorbance and Reflectance Measurement of Hemeproteins on Collagen. The concentration of met-aquo Mb and rHbI stock solution was determined by the rearrangement of the Beer-Lambert law equation, $c = A/\varepsilon b$, where c is the protein concentration (mM), A is the sample absorbance (unitless), b is the sample light path length (1 cm), and ε is the extinction coefficient for the particular proteins. For met-aquo Mb, met-aquo rHbI, and the rHbI-H_2S complex, the extinction coefficient was 188 cm^{-1} M^{-1} at 407 nm, 178 cm^{-1} M^{-1} at 407 nm, and 102 cm^{-1} M^{-1} at 426 nm, respectively [46, 47]. UV-Vis absorbance measurements were performed using a Shimadzu UV 2700 spectrophotometer.

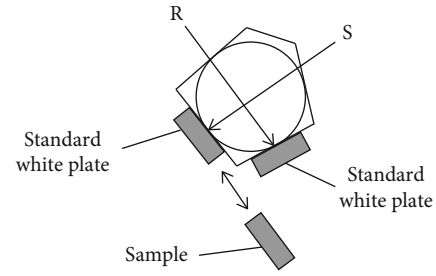

Figure 2: Setup for the measurement of diffuse reflectance.

The UV-Vis diffuse reflectance measurements of the hemeprotein collagen scaffold spot were monitored using the Shimadzu UV 2700 spectrophotometer equipped with an MPC 2600 unit, providing accurate reflectance measurements of hemeprotein on collagen. Figure 2 shows the standard plate setup on the reference (R) and sample (S) sides. Barium sulfate powder on both sides was used as a standard white plate to execute the diffuse reflectance baseline correction. The immobilized protein then replaced the S side to start data collection. Collagen sponges were mounted on the instrument, but only the center of the strip was exposed to radiation. The spectra were collected employing an incident angle of 0 degrees, a photomultiplier with 5.0 nm slit-width, 0.5 nm sampling pitch, 0.1 nm resolution, and six scans. A relation between the Kubelka-Munk function obtained from diffuse reflectance measurement has been described in the literature [48–50]. Therefore, all acquired reflectance spectra were converted using a Kubelka-Munk function by the UVProbe 2.3 software (Shimadzu Corporation). The Kubelka-Munk function represents the UV-Vis diffuse reflectance measurements, $F(R) = (1 - R)^2/2R$, where R is the experimental reflectance intensity [51–54].

Diffuse reflectance data were obtained for met-aquo Mb and met-aquo rHbI collagen scaffold in two different scenarios. First, the spectra were acquired on the collagen sample 30 minutes after the added hemeprotein drop solution. Then, these samples were stored at 4°C for 24 hours, and diffuse reflectance data were collected. In both circumstances, the spectra were the same. Next, the rHbI-H_2S complex on the collagen scaffold was prepared by reacting the immobilized met-aquo rHbI with hydrogen sulfide. Finally, the diffuse reflectance data was converted to the Kubelka-Munk function, facilitating monitoring of the transformation of met-aquo rHbI to rHbI-H_2S. The hydrogen sulfide heme complex is evidenced by the decreased intensity of the met-aquo rHbI 407 nm transition and the increased 426 nm band of rHbI-H_2S derivatives. Also, the electronic transitions of rHbI-H_2S species at 542 nm and 574 nm support the complex formation [47, 55]. All the experiments were conducted in triplicate.

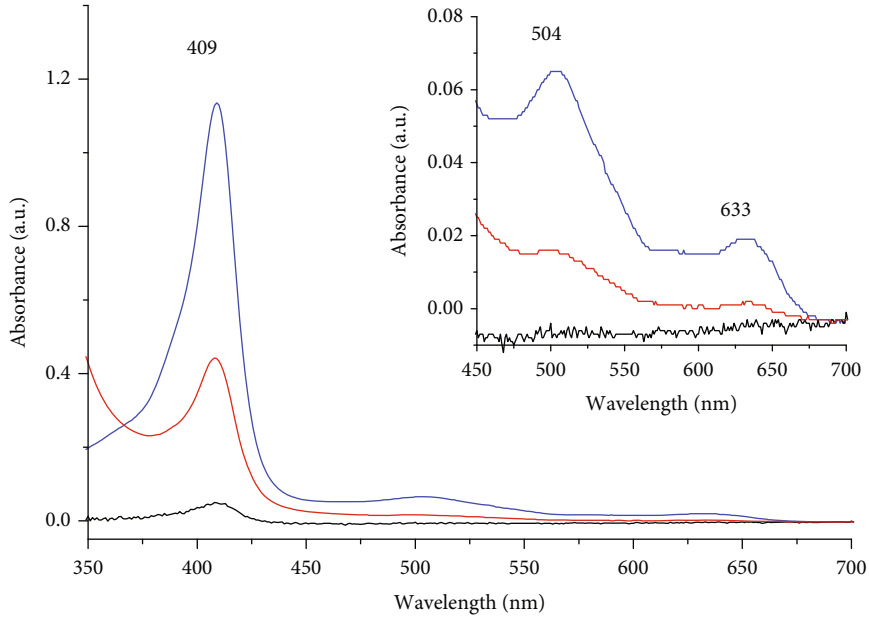

Figure 3: Comparison between the absorbance for 6 μM met-aquo Mb solution (blue line) with the immobilized protein on collagen measured by reflectance (red line) and absorption (black line). The inset shows a clearer view of the 450-700 nm region.

3. Results and Discussion

3.1. Absorbance and Reflectance of Hemeproteins on Collagen Sponge. Our study took advantage of the conventional UV-Vis spectroscopy used to measure absorbance in solutions with the UV-Vis coupled to reflection measurements of solid samples. Figure 3 shows UV-Vis absorption spectra of 6 μM met-aquo Mb in solution (blue line) and immobilized on collagen sponge (black line). The inset shows a view of the 450-700 nm region. The results indicate that with identical met-aquo Mb concentrations (6 μM), there is a significant intensity change between the UV-Vis absorption spectrum of the hemeprotein solution (blue line) and the collagen sponge (black line). Attempts were made to improve the absorbance intensity of the met-aquo Mb on the collagen sponge by subtracting a blank collagen sponge. Still, it did not improve the sample signal significantly. The variation in absorption can be attributed to the clearness between the hemeprotein in solution versus the collagen scaffold environment. Although the protein concentration on the collagen spot was not directly calculated, the initial hemeprotein content was identical to the solution concentration. Furthermore, the same immobilized met-aquo Mb sample was used to obtain the UV-Vis absorption (black line) and the reflection data, translated with the Kubelka-Munk function (Figure 3, red line). The data clearly shows that the UV-Vis diffuse reflectance spectroscopy significantly improves the band intensity in the sample. The observation suggests that processes and reactions of hemeproteins that adsorb collagen sponges can be monitored using diffuse reflectance techniques. Also, the identical electronic transitions between met-aquo Mb in solution and adsorbed on collagen at 409, 504, and 633 nm reveal that the heme chromophore pocket structure was preserved. The data also suggests that the surface did not interfere with the characteristic bands of the heme protein active center.

The results show that collagen with immobilized heme proteins had an average spot thickness of 0.041 cm. Therefore, the appropriate thickness should be determined to prevent loss of reflected radiation and avoid misinterpretation of results. This finding supports previous research where the diffuse reflectance revealed a significant depth dependency [56, 57]. Although reflectance is a limited measurement of the superficial analysis, with a penetration depth from 0.5 to 7 mm [52, 58, 59], it still depends on the optical absorption and scattering of the selected surface [57, 58]. The role of immobilized sample wetness versus 24 hours dried environments was evaluated by monitoring variations in the intensity of the UV-Vis reflectance measurements. The spectra were the same in both circumstances, and no significant changes in the linear regression were observed. These results agree with the diffuse reflectance measurements to quantify the met-aquo Mb of a wet meat sample [52] and share similarities with analysis in dry conditions of human skin *in vivo* [60]. Nevertheless, a slight increase in the slope for the freshly immobilized sample revealed that the water content in the protein spot reflected the light, increasing the reflectance signal [61]. Consequently, it demonstrated that the water content had a small influence in the 350-700 nm region measures because it altered the light path length [56].

3.2. Hemeprotein Distribution on a Collagen Scaffold. Figure 4(a) illustrates the four (4) sites of an expanded drop solution containing 12 μM met-aquo Mb added to a collagen surface. The hemeprotein distribution from the center was evaluated by diffuse reflectance. Figure 4(b) shows reflectance (%) plotted against wavelength, while Figure 4(c) represents the conversion to the Kubelka-Munk function for every colored site. Characteristic bands are typical of those expected for the met-aquo myoglobin derivative, evidencing

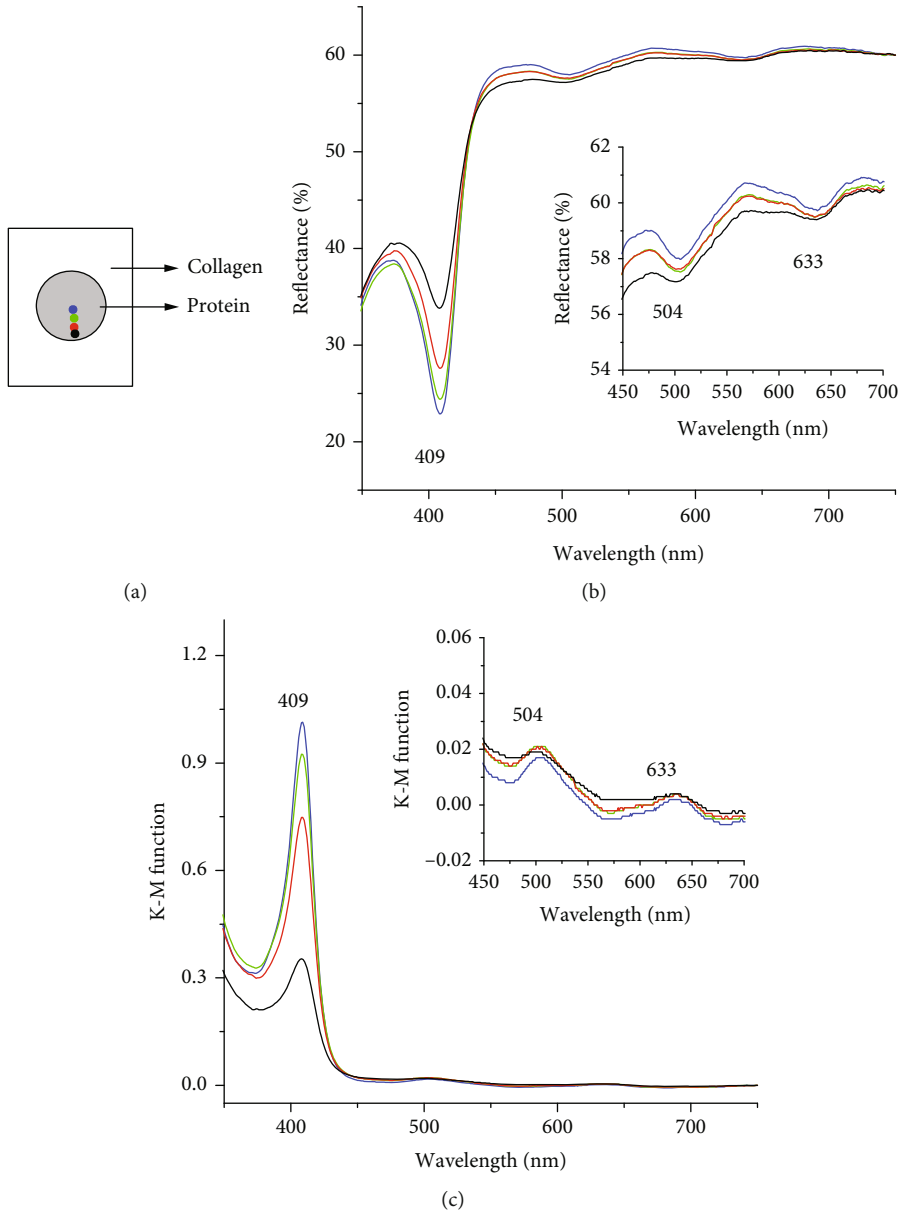

Figure 4: (a) Scheme of the 12 μM met-aquo Mb added to collagen. Colored circles represent the monitored positions. (b) UV-Vis diffuse reflectance measures and (c) the Kubelka-Munk function obtained from measured diffuse reflectance for their respective colored spots. The insets show an expanded view of the 450-700 nm range.

that the chromophore retained its optical properties. The spectrum with less percent reflectance (blue line) and the intense peaks can be associated with higher protein concentration [58]. The spectrum with a lower transition intensity (black line) was associated with measures obtained at the edge of the spot, with less chromophore. The hemeprotein single drop spread on the collagen revealed irregularities in the sample path length. In reflectance measurements, it is challenging to control path length, which could depend on the concentration of the sample [62]. A highly concentrated sample could result in short average path lengths, while the average path length will increase if the sample has a low concentration. As a consequence, quantitative analysis must be interpreted with caution. Thus, the evidence points out that the measurements should be performed close to the protein's deposition site to decrease systematic errors and misunderstandings in quantitative analysis.

3.3. Diffuse Reflectance of Recombinant met-aquo rHbI on Collagen Sponge. Spectral analysis of rHbI on a collagen sponge was performed by monitoring the intensity of the UV-Vis diffuse reflectance as a function of the hemeprotein concentration. Figure 5 shows reflectance converted to absorbance using the Kubelka-Munk function for various met-aquo rHbI solutions immobilized in collagen sponges. There is an intense band at 407 nm and small intensity bands at 502 and 633 nm [55]. The higher energy transition is approximately ten times more intense than the lower energy bands. This behavior is similar

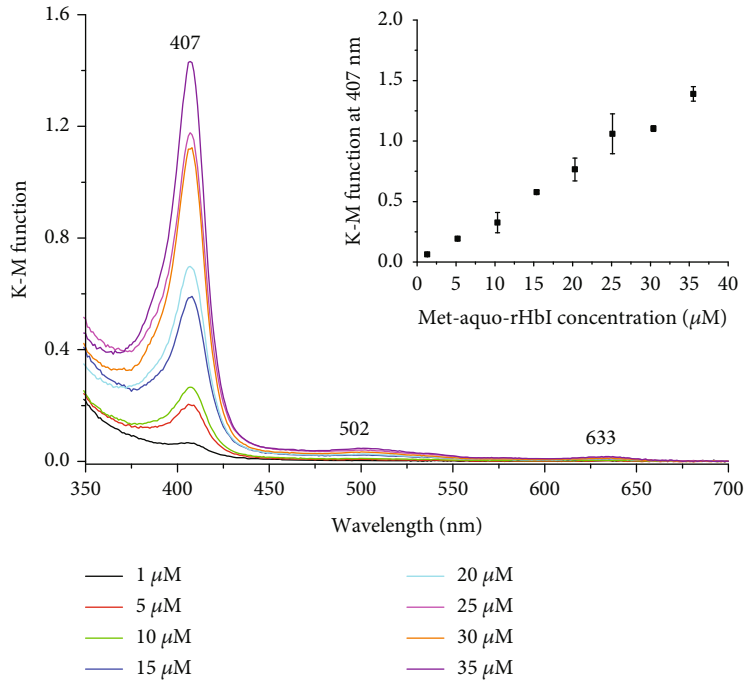

Figure 5: Spectra of diffuse reflectance transformation for different concentrations (1 to 35 μM) of immobilized met-aquo rHbI on collagen sponge. The inset shows variation in absorbance at 407 nm in each concentration showing a linear fit.

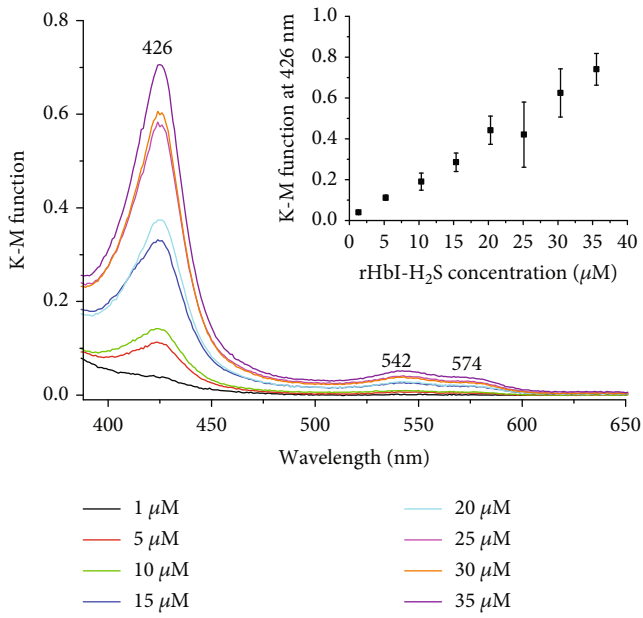

Figure 6: Spectra of rHbI-H_2S at different concentrations on the surface of the collagen sponge. Inset shows the changes in Kubelka-Munk units at 426 nm transition from the rHbI-H_2S complex against met-aquo rHbI concentration.

to that of the protein in the solution. These bands are attributed to $\pi \rightarrow \pi *$ electronic transitions of the heme porphyrin being sensitive to the heme oxidation, spin, and coordination states [63]. Thus, the evidence denotes that the HbI preserved its optical properties upon immobilization, suggesting that the heme porphyrin remains stable. These results are consistent with the work done on a slightly different assembly of immobilized myoglobin on collagen studied by UV spectroscopy and electrochemistry [64]. The met-aquo rHbI was analyzed in absorbance from 0.1 to 1.2. An $R^2 = 0.9987$ in concentrations ranging from 1 μM to 35 μM established a linear correlation between K-M function and met-aquo rHbI supported on collagen (Figure 5, inset). These results coincided with earlier findings where UV-Vis diffuse reflectance was implemented to quantify mercury in water [65] and myoglobin derivatives in pork and beef [52]. The standard deviation of 0.003 to 0.2 indicates that the data points are close to the mean and exhibit low spreading.

3.4. rHbI-H_2S Complex Formation on a Collagen Scaffold. The hydrogen sulfide solution (482 μM) reacts with the met-aquo rHbI collagen scaffold concentrations from 1 to 35 μM to generate a hemeprotein to H_2S ratio of 482 to 14. The range was chosen to ensure the reactivity of H_2S with met-aquo rHbI to create the rHbI-H_2S complex. If necessary, individual complex concentrations could be determined using a molar absorptivity coefficient of 102 cm^{-1} mM^{-1} [47]. Figure 6 shows the 426 nm, 542 nm, and 574 nm electronic transition characteristic of the six coordinated low spin ferric rHbI-H_2S complexes. Therefore, the data shows that the protein chromophore conformation was preserved after immobilization [47]. A linear correlation ($R^2 = 0.9916$) shown in the inset reflected an association between diffuse reflectance measurements and protein concentrations. The standard deviation range was ±0.004 to 0.2, having the most significant deviation at a higher concentration of the rHbI-H_2S complex. Various factors can influence the diffuse reflectance measurements, including beam penetration depth and high hemoglobin I concentration [66].

The data shows that 482 fold of H_2S to hemeprotein ratio did not produce deoxy heme Fe^{II} species, characterized by the Soret transition at 436 nm and dependent on H_2S concentration [45, 67, 68]. The reduction could not be observed because the transition was weak and may have remained inside the 426 nm envelope. The formation of the deoxy heme Fe^{II} species could have been prevented because the reaction was done aerobically [68, 69], causing a smaller than expected H_2S concentration. Also, the collagen matrix may have been stabilizing the rHbI-H_2S complex independently of the hydrogen sulfide concentration. However, the rHbI-H_2S formation clearly shows a linear dependence of the diffuse reflectance intensities and the rHbI-H_2S complex formation. Therefore, recombinant hemoglobin I on a collagen scaffold could act as a hydrogen sulfide scavenger, whose complex concentration can be determined using UV-Vis diffuse reflectance spectroscopy.

4. Conclusions

In our approach, met-aquo Mb and rHbI-H_2O were absorbed on a collagen porous scaffold and analyzed using UV-Vis absorption and diffuse reflectance spectroscopy. The techniques also evaluated the reaction between met-aquo rHbI and H_2S to generate a stable rHbI-H_2S complex on the scaffold moiety. These measures were then transformed to absorbance by the Kubelka-Munk function, which conserved the same peaks as in hemeprotein solution. These results suggest that the hemeproteins active center was not affected upon insertion into the collagen scaffold. Furthermore, the hydrogen sulfide concentration ratio to rHbI-H_2O (1-35 μM) was 482 to 14 shows a linear behavior between the K-M function and heme protein concentration. Overall, the results demonstrate the ability of the rHbI-H_2O collagen composite to be an excellent trap for H_2S by forming the rHbI-H_2S complex due to its extraordinary affinity for H_2S (k_{on} 6.8×10^3 M^{-1} s^{-1}/k_{off} 5.5×10^{-5} s^{-1}) of (1.24×10^8 M^{-1}). Hence, met-aquo rHbI is exceptionally suitable for the detection of H_2S [20]. The results also suggest that the process is a direct function of the rHbI-H_2O concentration present in the scaffold collagen system. Future work in this direction includes producing a met-aquo rHbI collagen gel capable of being printed as single drops in polymer, cotton, or chromatographic paper, as has been done for other chemical systems [25, 70, 71]. The process determines H_2S gas concentrations from different biological sources by measuring the rHbI-H_2S concentration in the single drop moiety, using UV-Vis diffuse reflectance techniques, which are simple, nondestructive, and low-cost tools. Although further research is needed, the design of rHbI-H_2S-collagen as an H_2S donor can extend their use to new therapeutic prospects.

Data Availability

The data used to support the findings of this study are included within the article. Additional information is available upon request by Jennifer Vargas Santiago.

Conflicts of Interest

The authors declare that they have no conflicts of interest.

Acknowledgments

This research was supported by PR-INBRE NIH/NIGMS under Grant No. P20GM103475. In addition, we recognize the support of the Alfred Sloan Foundation. Finally, we are grateful for the guidance provided by the Graduate Writing Facilitators of the Graduate Research and Innovation Center (GRIC) at the University of Puerto Rico-Mayagüez.

Supplementary Materials

Scheme of the immobilization of the hemoglobin I on the surface of a collagen sponge and the measurement of reflectance. *(Supplementary Materials)*

References

[1] J. Jiang, A. Chan, S. Ali et al., "Ultrastructural characterization of the lower motor system in a mouse model of Krabbe disease," *Scientific Reports*, vol. 6, no. 1, pp. 1–10, 2016.

[2] P. Haouzi, T. Sonobe, and A. Judenherc-Haouzi, "Hydrogen sulfide intoxication induced brain injury and methylene blue," *Neurobiology of Disease*, vol. 133, article 104474, 2020.

[3] S. Yuan, C. G. Kevil, S. Rajendran, X. Shen, J. Glawe, and G. K. Kolluru, "Nitric Oxide and Hydrogen Sulfide Regulation of Ischemic Vascular Growth and Remodeling," *Comprehensive Physiology*, vol. 9, pp. 1213–1247, 2019.

[4] K. R. Olson, "Is hydrogen sulfide a circulating "gasotransmitter" in vertebrate blood?," *Biochimica et Biophysica Acta (BBA)-Bioenergetics*, vol. 1787, no. 7, pp. 856–863, 2009.

[5] R. Wang, "Physiological implications of hydrogen sulfide: a whiff exploration that blossomed," *Physiological Reviews*, vol. 92, no. 2, pp. 791–896, 2012.

[6] M. R. Hellmich, C. Coletta, C. Chao, and C. Szabo, "The therapeutic potential of cystathionine β-synthetase/hydrogen sulfide inhibition in cancer," *Antioxidants Redox Signal*, vol. 22, no. 5, pp. 424–448, 2015.

[7] G. Renieris, K. Katrini, C. Damoulari et al., "Serum hydrogen sulfide and outcome association in pneumonia by the SARS-CoV-2 Coronavirus," *Shock*, vol. 54, no. 5, pp. 633–637, 2020.

[8] J. L. Wallace and R. Wang, "Hydrogen sulfide-based therapeutics: exploiting a unique but ubiquitous gasotransmitter," *Nature Reviews. Drug Discovery*, vol. 14, no. 5, pp. 329–345, 2015.

[9] E. Zaorska, L. Tomasova, D. Koszelewski, R. Ostaszewski, and M. Ufnal, "Hydrogen sulfide in pharmacotherapy, beyond the hydrogen sulfide-donors," *Biomolecules*, vol. 10, no. 2, p. 323, 2020.

[10] M. Whiteman, S. Le Trionnaire, M. Chopra, B. Fox, and J. Whatmore, "Emerging role of hydrogen sulfide in health and disease: critical appraisal of biomarkers and pharmacological tools," *Clinical Science*, vol. 121, no. 11, pp. 459–488, 2011.

[11] S. Y. Peng, X. Wu, T. Lu, G. Cui, and G. Chen, "Research progress of hydrogen sulfide in Alzheimer's disease from laboratory to hospital: a narrative review," *Medical Gas Research*, vol. 10, no. 3, pp. 125–129, 2020.

[12] B. V. Nagpure and J.-S. Bian, "Brain, learning, and memory: role of H_2S in neurodegenerative diseases," *Chemistry, biochemistry and pharmacology of hydrogen sulfide*, vol. 230, pp. 193–215, 2015.

[13] F. S. Quan and G. J. Lee, "Analytical Methods for Detection of Gasotransmitter Hydrogen Sulfide Released from Live Cells," *BioMed Research International*, vol. 2021, Article ID 5473965, 14 pages, 2021.

[14] A. Boffi, M. Rizzi, F. Monacelli, and P. Ascenzi, "Determination of H_2S solubility via the reaction with ferric hemoglobin I from the bivalve mollusc Lucina pectinata," *Biochimica et Biophysica Acta (BBA)-General Subjects*, vol. 1523, no. 2-3, pp. 206–208, 2000.

[15] G. Schiavon, G. Zotti, R. Toniolo, and G. Bontempelli, "Electrochemical detection of trace hydrogen sulfide in gaseous samples by porous silver electrodes supported on ion-exchange membranes (solid polymer electrolytes)," *Analytical Chemistry*, vol. 67, no. 2, pp. 318–323, 1995.

[16] N. S. Lawrence, J. Davis, F. Marken et al., "Electrochemical detection of sulphide: a novel dual flow cell," *Sensors and Actuators B: Chemical*, vol. 69, no. 1-2, pp. 189–192, 2000.

[17] N. S. Lawrence, L. Jiang, T. G. J. Jones, and R. G. Compton, "A thin-layer amperometric sensor for hydrogen sulfide: the use of microelectrodes to achieve a membrane-independent response for Clark-type sensors," *Analytical Chemistry*, vol. 75, no. 10, pp. 2499–2503, 2003.

[18] P. Jeroschewski, C. Steuckart, and M. Kühl, "An amperometric microsensor for the determination of H_2S in aquatic environments," *Analytical Chemistry*, vol. 68, no. 24, pp. 4351–4357, 1996.

[19] J. E. Doeller, T. S. Isbell, G. Benavides et al., "Polarographic measurement of hydrogen sulfide production and consumption by mammalian tissues," *Analytical Biochemistry*, vol. 341, no. 1, pp. 40–51, 2005.

[20] E. Collazo, R. Pietri, W. De Jesús et al., "Functional characterization of the purified holo form of hemoglobin I from Lucina pectinata overexpressed in Escherichia coli," *The Protein Journal*, vol. 23, no. 4, pp. 239–245, 2004.

[21] M. Ortega-Núñez, R. J. Tremont, C. A. Vega-Olivencia, and J. López-Garriga, "Electrochemistry of Hemoglobin I from Lucina Pectinata immobilized on a modified gold electrode with 3-mercaptopropionic acid," *International Journal of Analytical and Bioanalytical Chemistry*, vol. 2, pp. 218–227, 2012.

[22] L. Torres-González, R. Díaz, C. A. Vega-Olivencia, and J. López-Garriga, "Characterization of recombinant his-tag protein immobilized onto functionalized gold nanoparticles," *Sensors*, vol. 18, no. 12, pp. 42615–42621, 2018.

[23] R. Díaz-Ayala, L. Torres-González, R. Pietri, C. R. Cabrera, and J. López-Garriga, "Engineered (Lys)6-tagged recombinant sulfide-reactive hemoglobin I for covalent immobilization at multiwalled carbon nanotubes," *ACS Omega*, vol. 2, no. 12, pp. 9021–9032, 2017.

[24] Y. J. Ahn, Y. J. Lee, J. Lee, D. Lee, H. K. Park, and G. J. Lee, "Colorimetric detection of endogenous hydrogen sulfide production in living cells," *Spectrochimica Acta Part A: Molecular and Biomolecular Spectroscopy*, vol. 177, pp. 118–124, 2017.

[25] J. Lee, Y. J. Lee, Y. J. Ahn, S. Choi, and G. J. Lee, "A simple and facile paper-based colorimetric assay for detection of free hydrogen sulfide in prostate cancer cells," *Sensors and Actuators B: Chemical*, vol. 256, pp. 828–834, 2018.

[26] J. Zeng, M. Li, A. Liu et al., "Au/AgI dimeric nanoparticles for highly selective and sensitive colorimetric detection of hydrogen sulfide," *Advanced Functional Materials*, vol. 28, article 1800515, 26 pages, 2018.

[27] J. Vargas-Santiago, J. López-Garriga, and J. Encapsulation Adsorpt, "Transfer and reactivity of hydrogen sulfide with immobilized hemeproteins in polymeric matrix," *Journal of Encapsulation and Adsorption Sciences*, vol. 9, no. 2, pp. 109–126, 2019.

[28] R. Ravichandran, J. G. Martinez, E. W. H. Jager, J. Phopase, and A. P. F. Turner, "Type I collagen-derived injectable conductive hydrogel scaffolds as glucose sensors," *ACS Applied Materials & Interfaces*, vol. 10, no. 19, pp. 16244–16249, 2018.

[29] F. Subhan, Z. Hussain, I. Tauseef, A. Shehzad, and F. Wahid, "A review on recent advances and applications of fish collagen," *Critical Reviews in Food Science and Nutrition*, vol. 61, no. 6, pp. 1027–1037, 2021.

[30] M. V. Bhuimbar, P. K. Bhagwat, and P. B. Dandge, "Extraction and characterization of acid soluble collagen from fish waste: development of collagen-chitosan blend as food packaging film," *Journal of Environmental Chemical Engineering*, vol. 7, no. 2, pp. 102983–102987, 2019.

[31] L. Cao, X. Qiu, Q. Jiao, P. Zhao, J. Li, and Y. Wei, "Polysaccharides and proteins-based nanogenerator for energy harvesting and sensing: a review," *International Journal of Biological Macromolecules*, vol. 173, pp. 225–243, 2021.

[32] C. Oostendorp, P. J. Geutjes, F. Smit et al., "Sustained Postnatal Skin Regeneration Upon Prenatal Application of Functionalized Collagen Scaffolds," *Tissue Engineering Part A*, vol. 27, no. 1-2, pp. 10–25, 2021.

[33] J. M. Lee, S. K. Q. Suen, W. L. Ng, W. C. Ma, and W. Y. Yeong, "Comparison study of the effects of cationic liposomes on delivery across 3D skin tissue and whitening effects in pigmented 3D skin," *Macromolecular Bioscience*, vol. 21, no. 5, pp. 2000413–2000418, 2021.

[34] S. Pradhan, A. K. Brooks, and V. K. Yadavalli, "Nature-derived materials for the fabrication of functional biodevices," *Materials Today Bio*, vol. 7, article 100065, 2020.

[35] S. Unser, S. Holcomb, R. Cary, and L. Sagle, "Collagen-gold nanoparticle conjugates for versatile biosensing," *Sensors (Switzerland)*, vol. 17, no. 2, pp. 311–378, 2017.

[36] E. Roussakis, R. V. Ortines, B. L. Pinsker et al., "Theranostic biocomposite scaffold membrane," *Biomaterials*, vol. 212, pp. 17–27, 2019.

[37] S. Zong, Y. Cao, Y. Zhou, and H. Ju, "Hydrogen peroxide biosensor based on hemoglobin modified zirconia nanoparticles-grafted collagen matrix," *Analytica Chimica Acta*, vol. 582, no. 2, pp. 361–366, 2007.

[38] Z. Zheng, A. Chen, H. He et al., "pH and enzyme dual-responsive release of hydrogen sulfide for disc degeneration therapy," *Journal of Materials Chemistry B*, vol. 7, no. 4, pp. 611–618, 2019.

[39] L. Gambari, E. Amore, R. Raggio et al., "Hydrogen sulfide-releasing silk fibroin scaffold for bone tissue engineering," *Materials Science and Engineering: C*, vol. 102, pp. 471–482, 2019.

[40] R. Raggio, W. Bonani, E. Callone et al., "Silk fibroin porous scaffolds loaded with a slow-releasing hydrogen sulfide agent (GYY4137) for applications of tissue engineering," *ACS Biomaterials Science & Engineering*, vol. 4, no. 8, pp. 2956–2966, 2018.

[41] I. Cacciotti, M. Ciocci, E. Di Giovanni, F. Nanni, and S. Melino, "Hydrogen sulfide-releasing fibrous membranes: potential patches for stimulating human stem cells proliferation and viability under oxidative stress," *International Journal of Molecular Sciences*, vol. 19, no. 8, p. 2368, 2018.

[42] A. M. Al-Bishari, K. H. R. Yie, M. A. Al-Baadani et al., "JK-2 loaded electrospun membrane for promoting bone regeneration," *Materials Science and Engineering: C*, vol. 130, article 112471, 2021.

[43] R. V. Pinto, S. Carvalho, F. Antunes, J. Pires, and M. L. Pinto, "Front Cover: Fabulous at Fifteen! (ChemMedChem 1/2021)," *ChemMedChem*, vol. 16, no. 1, pp. 1–26, 2021.

[44] R. G. León, H. Munier-Lehmann, O. Barzu et al., "High-level production of recombinant sulfide-reactive hemoglobin I from *Lucina pectinata* in *Escherichia coli*: High yields of fully functional holoprotein synthesis in the BLi5 *E. coli* strain," *Protein expression and purification*, vol. 38, pp. 184–195, 2004.

[45] R. Pietri, A. Lewis, R. G. León et al., "Factors controlling the reactivity of hydrogen sulfide with hemeproteins," *Biochemistry*, vol. 48, no. 22, pp. 4881–4894, 2009.

[46] E. Antonini and M. Brunori, "Hemoglobin and myoglobin in their reactions with ligands," *Frontiers of biology*, vol. 21, pp. 27–31, 1971.

[47] D. W. Kraus, J. B. Wittenberg, L. Jing-fen, and J. Peisach, "Hemoglobins of the Lucina pectinata/bacteria symbiosis. II. An electron paramagnetic resonance and optical spectral study of the ferric proteins," *The Journal of Biological Chemistry*, vol. 265, no. 27, pp. 16054–16059, 1990.

[48] P. Tziourrou, J. Vakros, and H. K. Karapanagioti, "Using diffuse reflectance spectroscopy (DRS) technique for studying biofilm formation on LDPE and PET surfaces: laboratory and field experiments," *Environmental Science and Pollution Research*, vol. 27, no. 11, pp. 12055–12064, 2020.

[49] M. K. Gunde, J. K. Logar, Z. C. Orel, and B. Orel, "Application of the Kubelka-Munk theory to thickness-dependent diffuse reflectance of black paints in the Mid-IR," *Applied Spectroscopy*, vol. 49, no. 5, pp. 623–629, 1995.

[50] K. R. Millington, "Diffuse reflectance spectroscopy of fibrous proteins," *Amino Acids*, vol. 43, no. 3, pp. 1277–1285, 2012.

[51] B. Hernández, C. Sáenz, C. Alberdi, and J. M. Diñeiro, "Comparison between two different methods to obtain the proportions of myoglobin redox forms on fresh meat from reflectance measurements," *Journal of food science and technology*, vol. 52, no. 12, pp. 8212–8219, 2015.

[52] T. Nguyen, S. Kim, and J. G. Kim, "Diffuse reflectance spectroscopy to quantify the met-myoglobin proportion and meat oxygenation inside of pork and beef," *Food Chemistry*, vol. 275, pp. 369–376, 2019.

[53] G. Kortüm, *Reflectance Spectroscopy: Principles, Methods, Applications*, Springer Science & Business Media, 2012.

[54] R. W. Frei and J. D. MacNeil, *Diffuse Reflectance Spectroscopy in Environmental Problem-Solving*, CRC Press, New York, 1973.

[55] J. B. Kraus and J. B. Wittenberg, "Hemoglobins of the Lucina pectinata/bacteria symbiosis. I. Molecular properties, kinetics and equilibria of reactions with ligands," *Journal of Biological Chemistry*, vol. 265, no. 27, pp. 16043–16053, 1990.

[56] P. A. Torzilli, A. Azimulla, and J. Biomed, "Ultraviolet light (365 nm) transmission properties of articular cartilage as a function of depth, extracellular matrix, and swelling," *Journal of Biomedical Materials Research Part A*, vol. 108, no. 2, pp. 327–339, 2020.

[57] M. Milosevic and S. L. Berets, "A review of FT-IR diffuse reflection sampling considerations," *Applied Spectroscopy Reviews*, vol. 37, no. 4, pp. 347–364, 2002.

[58] J. Q. Brown, K. Vishwanath, G. M. Palmer, and N. Ramanujam, "Advances in Quantitative UV-Visible Spectroscopy for Clinical and Pre-clinical Application in Cancer," *Current Opinion in Biotechnology*, vol. 20, pp. 119–131, 2009.

[59] J. H. Nilsson, N. Reistad, H. Brange, C. F. Öberg, and C. Sturesson, "Diffuse reflectance spectroscopy for surface measurement of liver pathology," *European Surgical Research*, vol. 58, no. 1-2, pp. 40–50, 2017.

[60] G. Zonios and A. Dimou, "Modeling diffuse reflectance from semi-infinite turbid media: application to the study of skin optical properties," *Optics Express*, vol. 14, no. 19, pp. 396–402, 2006.

[61] A. Hassoun, K. Heia, S.-K. Lindberg, and H. Nilsen, "Performance of Fluorescence and Diffuse Reflectance Hyperspectral Imaging for Characterization of Lutefisk: A Traditional Norwegian Fish Dish," *Molecules*, vol. 25, no. 5, p. 1191, 2020.

[62] H. E. Snyder, "Analysis of pigments at the surface of fresh beef with reflectance spectrophotometry," *Journal of Food Science*, vol. 30, no. 3, pp. 457–463, 1965.

[63] M. Gouterman, "Spectra of porphyrins," *Journal of Molecular Spectroscopy*, vol. 6, pp. 138–163, 1961.

[64] X. Miao, Y. Liu, W. Gao, and N. Hu, "Layer-by-layer assembly of collagen and electroactive myoglobin," *Bioelectrochemistry*, vol. 79, no. 2, pp. 187–192, 2010.

[65] C. Yin, J. Iqbal, H. Hu et al., "Sensitive determination of trace mercury by UV–visible diffuse reflectance spectroscopy after complexation and membrane filtration-enrichment," *Journal of Hazardous Materials*, vol. 233-234, pp. 207–212, 2012.

[66] F. M. Mirabella, "A critical evaluation of internal reflection spectroscopic methods for determining macromolecular orientation in polymer surfaces," *Applied spectroscopy*, vol. 42, pp. 1258–1265, 1998.

[67] J. A. Berzofsky, J. Peisach, and W. E. Blumberg, "Sulfheme proteins: I. Optical and magnetic properties of sulfmyoglobin and its derivatives," *The Journal of Biological Chemistry*, vol. 246, no. 10, pp. 3367–3377, 1971.

[68] S. Chaiprapat, R. Mardthing, D. Kantachote, and S. Karnchanawong, "Removal of hydrogen sulfide by complete aerobic oxidation in acidic biofiltration," *Process Biochemistry*, vol. 46, no. 1, pp. 344–352, 2011.

[69] K. R. Olson, "A case for hydrogen sulfide metabolism as an oxygen sensing mechanism," *Antioxidants*, vol. 10, no. 11, pp. 1630–1650, 2021.

[70] H. Zhang, C. Xia, G. Feng, and J. Fang, "Hospitals and Laboratories on Paper-Based Sensors: A Mini Review," *Sensors*, vol. 21, no. 18, p. 5998, 2021.

[71] D. J. McClements, "Encapsulation, protection, and delivery of bioactive proteins and peptides using nanoparticle and microparticle systems: a review," *Advances in Colloid and Interface Science*, vol. 253, pp. 1–22, 2018.